Cellulose (2021) 28:10609–10624
https://doi.org/10.1007/s10570-021-04206-w

ORIGINAL RESEARCH

# Synergetic effect of cationic starch (ether/ester) and Pluronics for improving inkjet printing quality of office papers

**Mohit Sharma · Roberto Aguado · Dina Murtinho · Artur J. M. Valente · Paulo J. T. Ferreira**

Received: 21 June 2021 / Accepted: 14 September 2021 / Published online: 23 September 2021


**Abstract** Improving the printability of paper is still a relevant challenge, despite the fast development of digital communications. While it is well-known that cationic starches enhance ink density, their commercial paper-grade forms are limited to ethers with low degree of substitution. This work addresses the underexplored potential of highly substituted cationic starch for paper coating and its combination with triblock polymers, namely Pluronics (P123 and F127), taking advantage of their supramolecular interactions with amylose chains. For that purpose, cationic starch ether and ester (starch betainate), both with a degree of substitution of 0.3, were synthesized by alkaline etherification and by transesterification, respectively. Paper without any surface treatment was subjected to one-side bar coating with suspensions encompassing those products and Pluronics, besides other common components. Black, cyan, yellow and magenta inks were printed on all coated papers through an inkjet printer. Key properties of printing quality such as the gamut area, gamut volume, optical density, print-through, inter-color bleed and circularity were measured in a controlled temperature-humidity environment. For instance, a formulation with cationic starch (ether/ester) and P123 improved the gamut area by 16–18% in comparison to native starch-coated paper sheets. Interestingly, the individual assessment of each component showed that cationic starch ether, starch betainate and P123 only improved the gamut area by 5.6%, 8.9% and 6.8%, respectively. Finally, but not less importantly, starch betainate was found to quench optical brightening agents to a lesser extent than cationic starch ethers.

**Supplementary Information** The online version contains supplementary material available at https://doi.org/10.1007/s10570-021-04206-w.

M. Sharma · P. J. T. Ferreira
CIEPQPF, Department of Chemical Engineering, University of Coimbra, Rua Sílvio Lima, Pólo II – Pinhal de Marrocos, 3030-790 Coimbra, Portugal

R. Aguado (✉) · D. Murtinho · A. J. M. Valente
CQC, Department of Chemistry, University of Coimbra, Rua Larga, PT, 3004-535 Coimbra, Portugal
e-mail: rag@uc.pt

## Graphic abstract

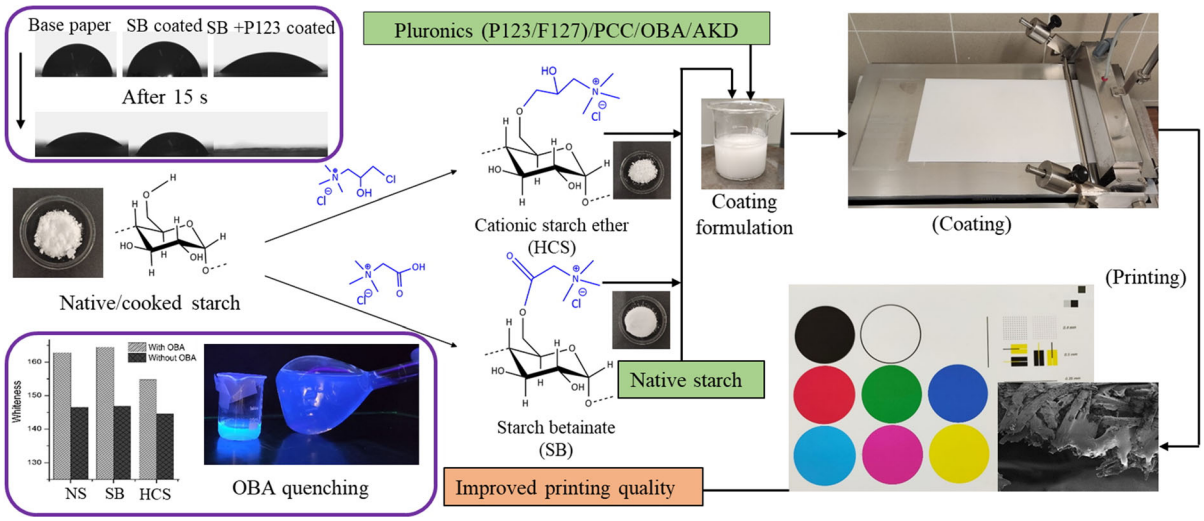


**Keywords** Cationic starch · Paper coating · Pluronics · Printing quality · Starch betainate · Whiteness

## Introduction

Paper coating formulations of printing and writing papers often comprise a number of different components such as pigments, surfactants, binders, thickeners, dispersants, crosslinkers, optical brightening agents (OBA), and/or lubricants. In each case, the composition depends on which objectives papermakers set for the end product. A careful selection of coating components can therefore be used to develop a paper surface with outstanding smoothness, enhanced barrier properties and, receiving less attention in the literature, improved printing properties (Sharma et al. 2020). Adsorption onto cellulosic fibers occurs when the paper surface is exposed to the coating suspension, but manufacturers cannot neglect the interactions between the components of such suspension, which take place beforehand, from the very moment they are mixed in an aqueous media. These interactions may include competitive adsorption, inclusion complex formation, and stabilization/destabilization (Sousa et al. 2014).

The inkjet printing properties of fine papers are majorly influenced by the surface properties thereof, such as charge, surface energy, roughness, permeability and surface strength (Bollström et al. 2013). A slight charge on the paper surface may lead to the effective immobilization of the ink pigments onto the coated paper surface, whereas a certain surface energy balance can favor a higher print density (Stankovská et al. 2014). Based on that, it has been shown that highly substituted cationic starch (HCS) has a significant positive effect on the ink holdout (Lee et al. 2002), optical density, whiteness, water fastness and ink fathering properties (Lamminmäki et al. 2011; Gigac et al. 2016a). These properties, along with the gamut area (GA), further increase in combination with amphiphilic polymers such as poly(vinyl alcohol) (Baptista et al. 2016), most probably due to ease of interpolymer diffusion of ink carriers during printing (Lamminmäki et al. 2011; Sousa et al. 2014).

While the biodegradability of native starch is obviously not under question, the biodegradability of its derivatives is too often taken for granted. It has been shown that HCS ethers lose biodegradability with increasing degree of substitution (DS), becoming non-biodegradable at DS $\geq$ 0.54 (Bendoraitiene et al. 2018). In this context, starch betainate (SB) rises as a convincing alternative, not only because betaine is naturally found, unlike conventional cationizing reagents, but also because the ester bonds of SB are

clearly more labile than ether bonds (Auzély-Velty and Rinaudo, 2003). Likewise, starch betainate (SB), a cationic starch ester, was suggested for the improvement of paper strength since the first work reporting its synthesis (Granö et al. 2000). However, as far as we know, no study has addressed the influence of SB on the printing properties of fine papers. This issue is addressed in the present work, evaluating coating formulations comprising SB and other interesting amphiphilic polymers, namely Pluronics.

Pluronics® is a BASF's trade name for the less commonly called poloxamers. This trade name comprises non-ionic, water-soluble, triblock copolymers of polyethylene oxide (PEO) and polypropylene oxide (PPO) units. Interestingly enough, they generally form inclusion complexes with starch in aqueous solution. This kind of binding has a significant effect on the dispersion performance and can be explained by hydrophobic interactions between hydrophobic parts of Pluronics macromolecules and the cavities of the amylose helix (Petkova-Olsson et al. 2017). Additionally, the micellar structure of these non-ionic surfactants also influences the adsorption onto the surface of cellulosic materials, which is enhanced in the presence of cationic polymers (Liu et al. 2010, 2011). Moreover, instead of becoming attached to the cellulosic substrate before printing, Pluronics can be directly included in the ink formulation, which is particularly useful for the inkjet printing of proteins (Mujawar et al. 2015).

In light of the aforementioned hypotheses and previous findings, paper sheets were coated using different concentrations of SB, HCS, Pluronics (P127 and F127), precipitated calcium carbonate (PCC), alkyl ketene dimer (AKD) and optical brightening agent (OBA). This study also illustrates the use of a statistical tool to design the coating experiments and to identify the most important factors to be considered for improving the paper printability. A comparison of HCS and SB coatings was also explored, discussing their influence on the whiteness of paper, given that the interaction between cationic polymers and OBAs, generally anionic, has been pointed out as a major cause of fluorescence quenching (Shi et al. 2012). All in all, this is the first work assessing the combination of cationic starches and Pluronics in paper coating, and it does so with an in-depth evaluation of their effects on optical, surface and printing properties.

## Materials and methods

### Materials

Native corn starch (NS), α-amylase (in standard buffer solution, pH 5.8), PCC, OBA and AKD were of industrial origin. 3-Chloro-2-hydroxypropyltrimethyl ammonium chloride (CHPTAC), Pluronics® P123 (MW $\sim$ 5750 g $mol^{-1}$, PEO $\sim$ 30 wt.% and CMC of 0.313 mM at 20 °C) (Alexandridis et al. 1994) and Pluronics® F127 (MW $\sim$ 12,600 g $mol^{-1}$, PEO-70 wt.% and CMC of 0.56 mM at 25 °C) (Thapa et al. 2020) were purchased from Sigma-Aldrich. Betaine hydrochloride (99%) was purchased from Alfa Aesar and used as-is for transesterification. All solvents were purified or dried prior to use the standard procedures. Other commercially available compounds were used without further purification.

Figure 1 schematizes the methods, highlighting the aforementioned materials and displaying all the steps taken towards coated and inkjet-printed paper sheets.

### Synthesis of HCS and SB

Native starch (NS) was mildly hydrolyzed with α-amylase (0.45 μL $g^{-1}$ of starch), under continuous stirring, at 80 °C for 5 min. The temperature was raised up to 90–95 °C for 15 min. Then, the starch solution was cooled down and absolute ethanol was added to precipitate the polysaccharide, hereinafter referred to as "cooked starch". Cooked starch was then vacuum filtered, dried and stored in an oven at 50 °C. This pretreatment is common to the synthesis of both HCS and SB.

HCS was synthesized as described elsewhere (Haack et al. 2002). Briefly, 10 g of cooked or native starch was converted into HCS using 33.5 mL of CHPTAC (60 wt.%) and 5.9 g of NaOH. The reaction was carried out for 24 h at 70 °C in 100 ml of distilled water. The reaction mixture was then neutralized with a 0.1% HCl solution.

Starch betainate (SB) was synthesized, as described in a previous paper (Sharma et al. 2021), through the transesterification of starch with methyl betainate (MeBetCl) in polar aprotic solvents. Briefly, 24 g of betaine hydrochloride was first esterified to synthesize MeBetCl using 11.3 mL of thionyl chloride and 75 mL of methanol, under reflux, for 4 h at 70 °C. MeBetCl was recovered through evaporation of

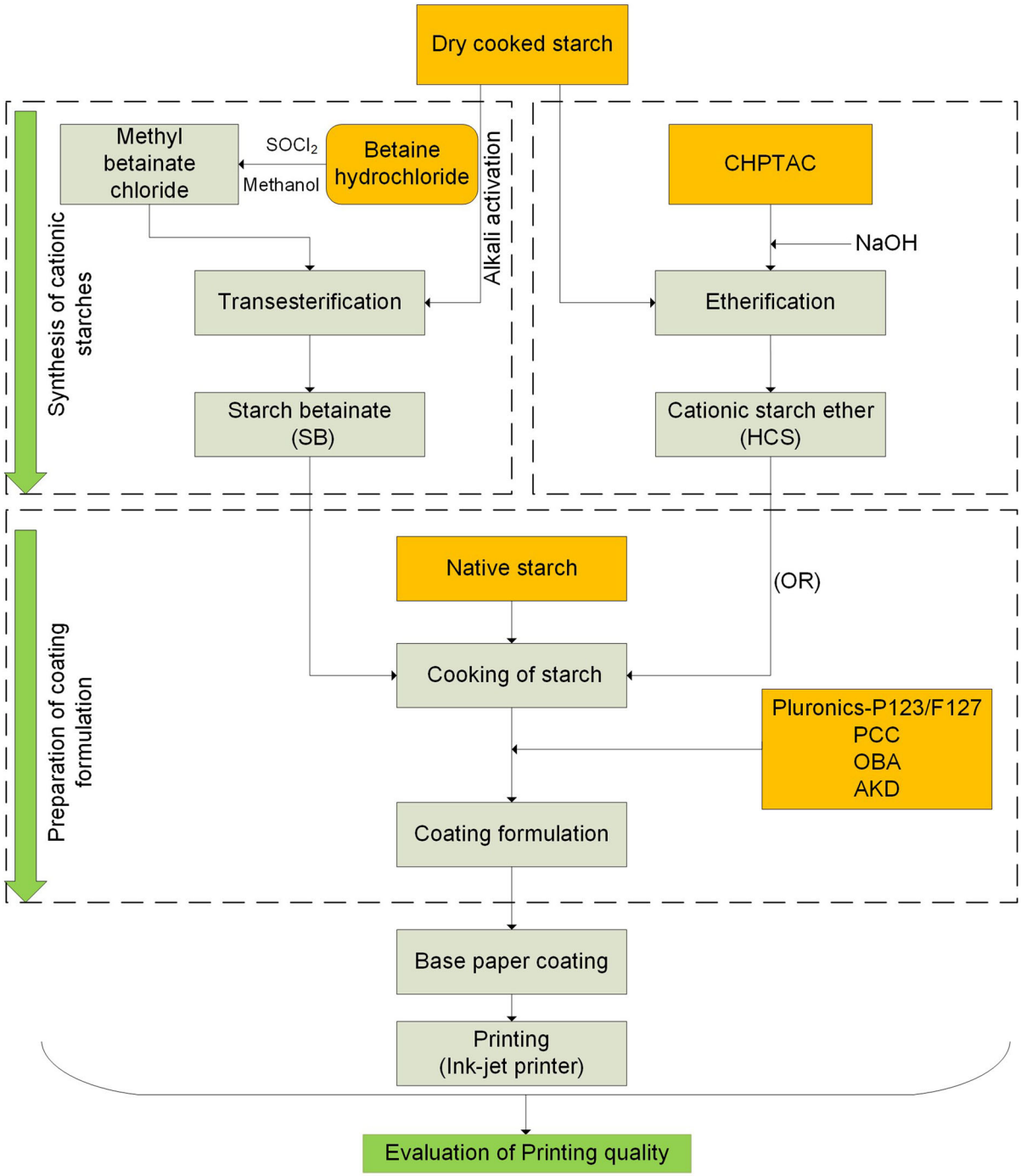


**Fig. 1** Outline of the experimental procedure

methanol followed by trituration in diethyl ether and, finally, the crude product was dried under high vacuum. Then, 10 g of cooked starch were converted into SB using 20.8 g of MeBetCl in *N,N*-dimethylformamide (DMF), 100 mL. Prior to transesterification, cooked starch was pre-activated in NaOH/ethanol. The reaction was carried out for 24 h at 70 °C.

HCS and SB were precipitated by adding ethanol (alcohol/water > 10, v/v), vacuum filtered and washed with absolute ethanol, followed by drying at 50 °C.

## Characterization of synthesized cationic starches

Attenuated Total Reflectance-Fourier Transform Infrared (ATR-FTIR) spectroscopy, $^{1}$H-nuclear magnetic resonance ($^{1}$H-NMR) spectroscopy and viscometry analysis were performed to characterize the synthesized cationic starches. ATR-FTIR spectra were recorded by using an Agilent Cary 630 spectrometer, from 750 to 3000 $cm^{-1}$, at a resolution of 4 $cm^{-1}$ and 64 scans per sample. NMR spectra were obtained from a Bruker Biospin GmbH spectrometer, at 400 MHz, using $D_2O$ as solvent. The degree of substitution was calculated from the area of the singlet assigned to the methyl protons of the quaternary ammonium group. The reliability of this result was confirmed by measuring the nitrogen percentage of samples on a Fisons Instruments EA 1108 CHNS-O elemental analyzer.

## Paper coating

NS was used as a common component for preparing all formulations in this work. For that, NS was cooked as described earlier, and then cooled down to 50 °C instead of precipitated. An industrial calendered uncoated paper (base paper, BP), produced from bleached eucalyptus kraft pulp with a basis weight of $\sim$ 78 g $m^{-2}$, was used as substrate for performing surface coating.

Coating of BP was performed using a Mathis laboratory coater, with a pre-drying infrared system coupled to an applicator bar (SVA-IR-B). The applicator roll with the diameter of 13 mm, in conjunction with a velocity of 6 m $min^{-1}$ and intermediate load at both sides, was used to achieve 1.5–3 g $m^{-2}$ per side, on the basis of dry coating weight. For all sheets, the coating time was 4 s/sheet. Afterwards, sheets were air dried at room temperature.

Besides NS, BP sheets were coated with SB, HCS, P123, F127, PCC, and combinations thereof. Coatings were performed using 8%, 16% and 24% of total solids coating weight of each of these components, and several combinations of them were tested at said concentrations. The coating compositions resulting from individual components (with NS) and combinations thereof are shown in Tables 1 and 2, respectively.

The surface weight gain was calculated by the difference between basis weights (ISO standard 536:1995) of the air-dried coated paper sheet and the respective BP sheet. Before characterization, all coated papers were kept at controlled temperature (23 °C ± 1) and humidity (RH 50% ± 2). For each run, three numbers for paper sheets were coated, printed and characterized for evaluating the printing quality.

## Paper properties

Bendtsen roughness (ISO 5636-3, 8791-2) and Gurley air permeability (ISO 5636/5) were measured for coated papers using appropriate testers from Frank-PTI. Whiteness (CIE W D65/10) of coated papers was measured using D65 illumination in the Elrepho spectrophotometer. The average value and the standard deviation of four independent measures are reported for Bendtsen roughness, Gurley permeability (also called Gurley porosity) and whiteness. The latter was related to the performance of OBA, as fluorescence emission spectra of solutions containing OBA were recorded by means of a FluoroMax 4 spectrofluorometer from Horiba.

Surface and cross-section micrographs of coated papers were obtained by means of a field emission scanning electron microscope (FE-SEM), Merlin (Carl Zeiss AG), including a Gemini II column and a secondary electron detector, and working at low acceleration voltage (2 kV). Furthermore, the average width of the coating layer was estimated by measuring the thickness of uncoated and coated paper sheets with a micrometer (ISO 534:1998).

### *Resistance to water*

The surface hydrophilicity for SB-coated papers was evaluated by contact angle goniometry. The static water contact angle (SWCA) was measured in an OCA 20 goniometer (Dataphysics, Germany) using the sessile drop method. A droplet of deionized water (10 μL) was automatically poured onto the coated paper surface. After settling, the formed angle was measured by fitting the Young–Laplace equation to the drop profile. Likewise, the dynamic water contact

**Table 1** Composition of coating components expressed as %w/w, on the basis of dry coating weight

| Ingredients | Coating formulations | | | | | | | | | | | | | |
|---|---|---|---|---|---|---|---|---|---|---|---|---|---|---|
| | HCS/SB | | | | P123 | | | F127 | | | PCC | | | Reference |
| HCS/SB | 8 | 16 | 24 | 16 | | | | | | | | | | |
| P123 | | | | | 8 | 16 | 24 | | | | | | | |
| F127 | | | | | | | | 8 | 16 | 24 | | | | |
| PCC | | | | | | | | | | | 8 | 16 | 24 | |
| OBA | 6 | 6 | 6 | | 6 | 6 | 6 | 6 | 6 | 6 | 6 | 6 | 6 | 6 |
| AKD | 0.4 | 0.4 | 0.4 | 0.4 | 0.4 | 0.4 | 0.4 | 0.4 | 0.4 | 0.4 | 0.4 | 0.4 | 0.4 | 0.4 |
| NS | 85.6 | 77.6 | 69.6 | 83.6 | 85.6 | 77.6 | 69.6 | 85.6 | 77.6 | 69.6 | 85.6 | 77.6 | 69.6 | 93.6 |

**Table 2** Composition of coating components for the interaction study, expressed as %w/w, on the basis of dry coating weight

| Ingredients | Coating formulations | | | | | | | | | |
|---|---|---|---|---|---|---|---|---|---|---|
| | HCS/SB + P123 | | | | HCS/SB + P123 + PCC | | | | Reference | |
| HCS/SB | 16 | 16 | 16 | 16 | 16 | 16 | 16 | 16 | | |
| P123 | 8 | 16 | 24 | 16 | 8 | 16 | 24 | 16 | | |
| PCC | | | | | 16 | 16 | 16 | 16 | | |
| OBA | 6 | 6 | 6 | | 6 | 6 | 6 | | 6 | |
| AKD | 0.4 | 0.4 | 0.4 | 0.4 | 0.4 | 0.4 | 0.4 | 0.4 | 0.4 | 0.4 |
| NS | 69.6 | 61.6 | 53.6 | 67.6 | 53.6 | 45.6 | 37.6 | 51.6 | 93.6 | 99.6 |

angle (DWCA) was measured over periods of up to 60 s.

The time profile of water penetration through coated samples was plotted by means of an EST Surface and Sizing Tester from Emtec. Briefly, this device monitors the ultrasound absorption or scattering at the air–water interfaces of small bubbles, since air flows out from the pores of the sheet as water penetrates through it.

*Viscosity and thermal degradation behavior*

The kinematic viscosity was determined using a size 100 Cannon–Fenske viscometer in a thermostatic bath (TAMSON TV 2000) set at 40 °C. Measurements followed the ISO 3105 standard. Polymer solutions were prepared with a concentration of 5 mg $cm^{-3}$ in 1 M NaOH/$H_2O$ (for HCS) and DMSO (for SB).

The thermogravimetric analysis (TGA) was carried out on a thermo-microbalance TG 209 F3 Tarsus, from Netzsch Instruments. Samples were heated from 40 to 600 °C, under a flow of nitrogen (20 mL $min^{-1}$), with a heating rate of 10 °C $min^{-1}$. TGA was performed for filter paper coated with P123, F127 and SB. A filter paper was cut into pieces (5 cm × 2 cm) and Pluronics P123/F127 were absorbed in this cellulosic substrate. This was carried out with a 10% Pluronic aqueous solution and a LayerBuilder dip coater from KSV. Cellulose substrates were dipped into the solution for 3 min, pulled out and air-dried. The same procedure was followed for 10% SB and 10% P123/F127 + 10% SB aqueous solutions.

Printing quality

Samples for measuring the printing quality were prepared as reported elsewhere (Lourenço et al., 2020). Briefly, the coated papers were printed using HP Officejet Pro 6230 inkjet printer in Max DPI mode (4800 × 1200 optimized DPI), having cyan, magenta, yellow, and black color ink cartridges. The printed sheets were air dried for 4 h under controlled conditions of temperature and humidity.

*Gamut area and gamut volume*

The GA is the area of the hexagon resulting from the $a^*$ and $b^*$ coordinates of six printed colors (red, green, blue, cyan, magenta, and yellow), where $a^*$ axis represents the color from green to red and axis $b^*$ represents the color from blue to yellow. It was determined by measuring the values of CIE $L^*a^*b^*$ coordinates for six color spots, including three base colors (cyan, magenta and yellow) and other three complimentary colors (red, green and blue). For that, the "X-Rite Eye One XTreme UV Cut" spectrophotometer was placed on each printed color spot, activating the UV light (D50, 2°). The readings were taken in the sequence of red, green, blue, cyan, magenta, and yellow color spots. Additionally, CIE $L^*a^*b^*$ values for black and white colors were measured to estimate the gamut volume (GV) of printed paper sheets.

*Optical density, print-through, inter-color bleed, and circularity*

In order to evaluate optical density (OD) and print-through (PT), the QEA PIAS-II spectrophotometer was used with a low-resolution optical module (33 μm/pixel with visual area of 21.3 mm × 16 mm), along with the software PIAS II, based on ISO 13660 quality standards, for processing the images. The PT of a printed paper requires the measurement of $L^*a^*b^*$ values on the opposite side of printed areas, in contrast with the non-printed area of the same paper sheet. The transmitted light intensity from a specific area of each color (black, white, cyan, magenta, and yellow) was measured using QEA PIAS-II, and thus PT and OD were calculated from the following equations:

$$\mathrm{OD} = \log_{10}(\text{Incident light/Transmitted light}) \quad (1)$$

$$\mathrm{PT} = \sqrt{(L_p^* - L_u^*)^2 + (a_p^* - a_u^*)^2 + (b_p^* - b_u^*)^2} \quad (2)$$

where $L^*$, $a^*$, $b^*$ are the CIE chromatic coordinates, and the subscripts $u$ and $p$ refer to areas of unprinted and back of the printed black spot, respectively.

The other printing properties, namely inter-color bleed (ITCB) and circularity (black), were also evaluated by means of QEA PIAS-II with high-resolution module (5 μm/pixel with 3.2 mm × 2.4 mm). This was used to measure the raggedness, which can be defined as the geometric distortion of the line and dots, given by the standard deviation of the residue from the lines and dots adjusted to their ideal limit. The higher the raggedness, the worse the ITCB and circularity.

*Statistical analysis*

In order to observe the interactions between coating components and their impact on the printing quality of coated papers, TIBCO's Statistica software was used as a statistical tool for the design of experiments and data analysis. In this study, four continuous factors, namely HCS, P123, PCC and OBA, were selected, each at two levels (0 and 16%), and a full factorial design with two center points was chosen to design the coating experiments. A total number of 18 runs were performed to evaluate the effect of these factors and their interactions on the printing quality, namely: GA; OD for cyan, magenta, yellow, and black; PT; ITCB and circularity for black color in the responses.

## Results and discussion

Synthesis of SB and HCS

Figure 2a presents the ATR-FTIR spectra for synthesized cationic starches from etherification and transesterification, using respectively CHPTAC and betaine hydrochloride, in comparison to the NS spectrum. The absorption peaks at 3300 $cm^{-1}$, 2912 $cm^{-1}$, 1648 $cm^{-1}$ can be assigned to the –OH, $–CH_2$ stretching vibrations, and $H_2O$ bending vibration due to water sorption, respectively. Additionally, peaks at 994 $cm^{-1}$ can be attributed to the ether bonds and the absorption band at 897 $cm^{-1}$ can be assigned to C1–H bending in starch. Compared to cooked starch, a new prominent peak at 1473 $cm^{-1}$ can be observed due to the quaternary ammonium group attached to the anhydroglucose unit (AGU) (Wang and Cheng 2009; Hebeish et al. 2010). Furthermore, the absorption band at 1750 $cm^{-1}$ is assigned to the ester bond in SB.

Figure 2b shows the $^1$H-NMR spectra for HCS and SB, compared to the spectrum of cooked starch. The singlet at 3.28 ppm is assigned to the nine hydrogens of methyl groups of the quaternary ammonium. The resonances from 3.5 to 4 ppm represent the hydrogens

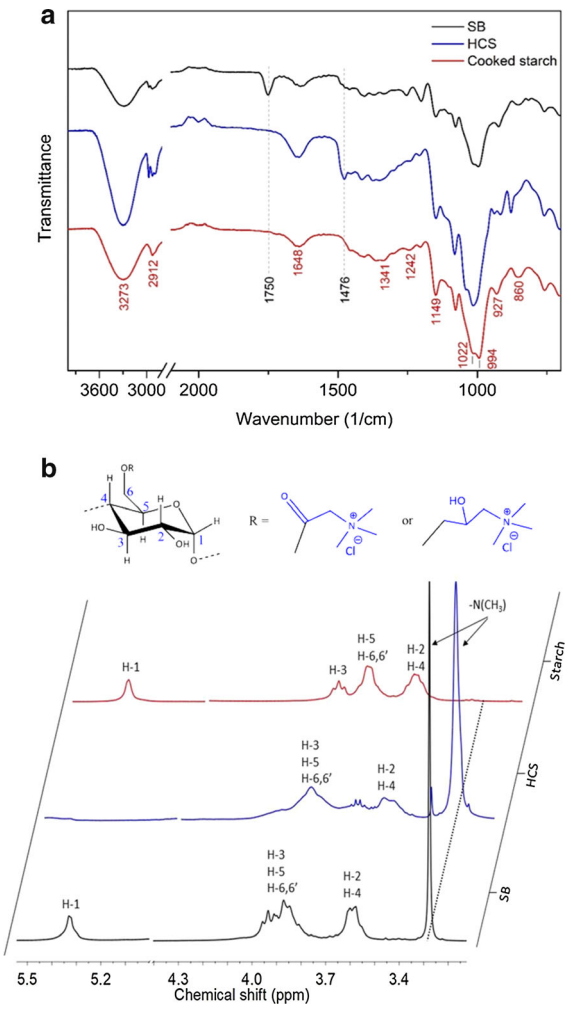


**Fig. 2** ATR-FTIR (**a**) and $^{1}$H-NMR (**b**) spectra for cationic starch ether and starch betainate, compared to cooked starch

attached to carbons 2, 4, 5, 6 (H-6 and H-6′), and 3 of AGU, typically in that order. The doublet for the H-1(α) anomeric proton lies downfield (5.35 ppm). There was a certain shift upfield and broadening of all signals upon cationization. No impurities were detected in SB, but the HCS spectrum displayed a singlet at 3.33 ppm and a quadruplet at 3.65 ppm, none of which belong to the canonical structure of cationic starches. The former could be due to quaternary ammonium groups arising from substitution on hydroxypropyl chains, instead of the hydroxyl groups of AGU.

An important hypothesis regarding the reaction is that enzymatic cooking improves its efficiency. Figure 3a shows the effect of cooking and reaction time on the DS of the synthesized HCS. It can be observed that the DS increases from 0.20 to 0.33 and from 0.34 to 0.43 with the increase in the reaction time from 3 to 24 h, when native and cooked starches were used as raw materials for the etherification reactions, respectively. This is likely due to the formation of more porous starch granules, which facilitates the access of the reagent to hydroxyl groups (Huber and BeMiller 2001). It was also observed that the cooking of starch enables the homogeneous dispersion of starch granules in the solvent by increasing the solubility and decreasing its viscosity, as seen in Fig. 3b (Gao et al. 2012).

Undoubtedly, due to the cleavage of 1–4 α-D-glucopyranosyl linkages of amylose and amylopectin, the inherent viscosity decreases with the enzymatic pre-treatment, from 199.4 $cm^3\ g^{-1}$ (NS) to 151.8 $cm^3\ g^{-1}$ (cooked starch). The viscosity was further reduced by 43–45% when using them in etherification. Likewise, the hydrolysis of starch molecules in highly alkaline media and at high temperature is evidenced by a loss of viscosity after functionalization. Nonetheless, after reaction times beyond 3 h, further hydrolysis is either negligible or compensated by the effects of cationization on polymer–solvent interactions.

Like etherification, the increase in DS and decreasing in viscosity were also observed in the synthesis of SB. However, DS increased much more abruptly, from 0.01 to 0.33, when using NS and cooked starch in the transesterification reaction, respectively, proving the poor reaction efficiency with NS. Given that the inherent viscosity decreased by ∼ 73%, starch faced higher depolymerization during functionalization, mostly due to the previous alkalization of starch at high temperature.

## Properties of coated sheets

Micrographs of BP and coated paper sheets are displayed in Fig. 4. None of those formulations involved PCC, so the characteristic hexagonal crystals that can be appreciated correspond to the starting material, i.e., PCC that had been added to the pulp before the formation of the paper web. As expected, the PCC particles close to the surface and nearby cellulosic fibers become strongly bound by HCS (Fig. 4b) and SB (Fig. 4d). Then, the addition of Pluronics, specifically P123, resulted in less binder (HCS and SB) at the surface (Fig. 4c and, more

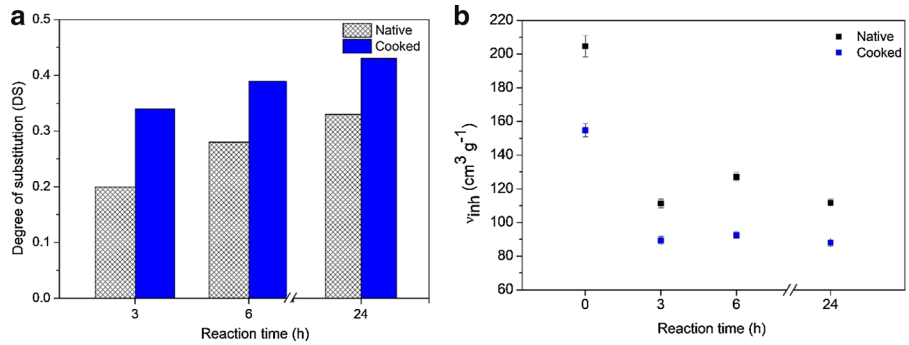


**Fig. 3** Effect of reaction time and enzymatic cooking on degree of substitution (**a**) and inherent viscosity (**b**) of HCS

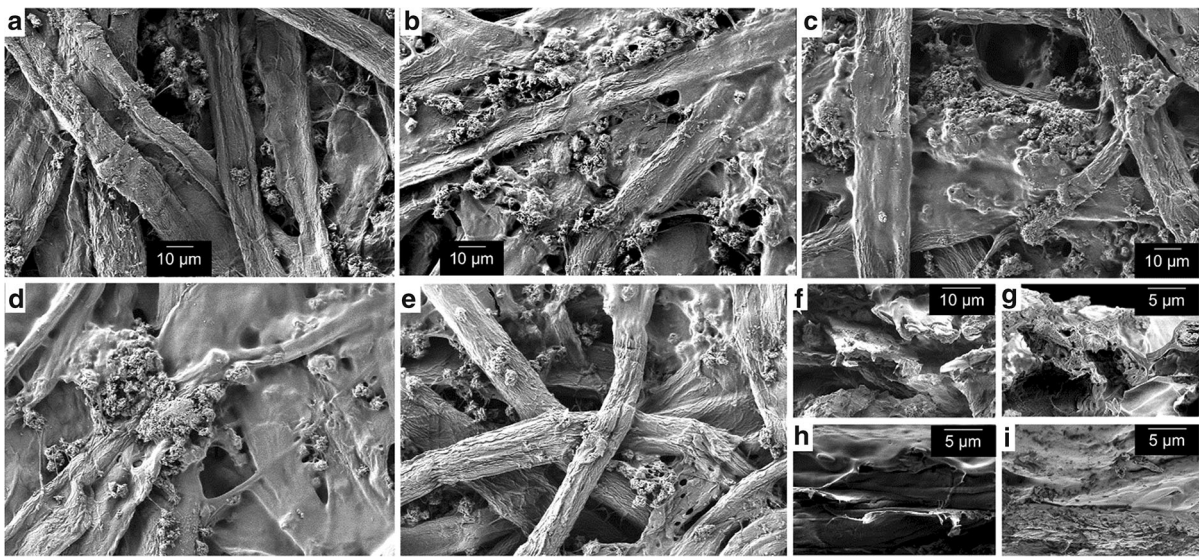


**Fig. 4** SEM images of the surface of uncoated paper (**a**), and of the surface (**b–e**) and cross-section (**f–i**) of paper sheets that underwent different surface treatments: with HCS (**b**, **f**), with HCS and P123 (**c**, **e**), with SB (**d**, **h**), and with SB and P123 (**e**, **i**)

clearly, 4e). Instead, the presence of this amphiphilic copolymer favors the penetration of binder through the cross-section of paper (Fig. 4f–i). This effect is more evident for SB, going from a thin layer over fibers (Fig. 4h) to an apparent depth of at least 15 µm (Fig. 4i). This is more than three times the nominal thickness gain of sheets, which is shown in Table 3.

Table 3 also displays the Bendtsen roughness, the Gurley permeability, and the SWCA values for papers coated with SB, Pluronics and/or PCC. For instance, addition of SB decreased the permeability of the paper surface and increased its smoothness. It can be appreciated that porosity was generally lower in the printed areas, although differences are not significant when P123 and SB were combined.

The static contact angle increased, although slightly, with SB or PCC. As intended, the interaction with non-ionic surfactants (Pluronics) decreased this angle. This increase in surface hydrophilicity was mimicked or even made more evident by the DWCA profiles and the water penetration plot (Figs. 5, S1 and S2). Through the process of wetting paper sheets coated with SB and Pluronics for 1 min, water drops reached contact angles below 5° after less than 20 s. Furthermore, liquid penetration was practically instantaneous when those sheets were immersed in water. Hence, Pluronics are expected to enhance the penetration, and thus fixation, of any polar ink.

In order to clarify the interactions between components, it should be noted that PCC, Pluronics, OBA

**Table 3** Properties of coated papers using different concentrations of SB, Pluronics (P123 and F127), and their combination in coating formulations

| | Conc. (%) | Roughness (mL/min) | Gurley(mL/min) | | SWCA (°) | Coating thickness (μm) | Whiteness | Gamut volume/$10^3$ | Weight gain ($g/m^2$) |
|---|---|---|---|---|---|---|---|---|---|
| | | | Unprinted | Printed | | | | | |
| Reference (NS) | | 329 ± 13 | 318 ± 07 | 320 | 72 ± 1 | 3 | 162.8 ± 1.3 | 132 ± 1 | 1.8 ± 0.3 |
| SB | 8 | 324 ± 14 | 379 ± 14 | 363 | 75 ± 2 | 4 | 162.3 ± 0.5 | 146 ± 1 | 2.5 ± 0.2 |
| | 16 | 311 ± 07 | 397 ± 04 | 364 | 77 ± 2 | 5 | 164.5 ± 0.3 | 151 ± 1 | 1.9 ± 0.2 |
| | 24 | 376 ± 09 | 420 ± 16 | 366 | 79 ± 1 | 4 | 164.1 ± 0.7 | 153 ± 1 | 2.3 ± 0.3 |
| P123 | 8 | 368 ± 09 | 407 ± 06 | 378 | 50 ± 3 | 5 | 165.1 ± 0.2 | 153 ± 1 | 2.9 ± 0.2 |
| | 16 | 379 ± 30 | 381 ± 05 | 368 | 43 ± 2 | 5 | 165.6 ± 0.2 | 152 ± 2 | 2.9 ± 0.1 |
| | 24 | 357 ± 09 | 354 ± 09 | 320 | 47 ± 1 | 6 | 165.8 ± 0.4 | 150 ± 2 | 3.0 ± 0.2 |
| F127 | 8 | 378 ± 38 | 356 ± 05 | 313 | 63 ± 3 | 4 | 163.6 ± 0.6 | 145 ± 2 | 2.4 ± 0.2 |
| | 16 | 363 ± 28 | 325 ± 50 | 325 | 57 ± 1 | 4 | 163.4 ± 0.4 | 141 ± 3 | 2.7 ± 0.1 |
| | 24 | 329 ± 18 | 444 ± 13 | 388 | 53 ± 2 | 6 | 162.2 ± 0.7 | 150 ± 1 | 2.7 ± 0.2 |
| PCC | 8 | 414 ± 37 | 347 ± 05 | 296 | 75 ± 2 | 3 | 160.9 ± 0.3 | 149 ± 1 | 2.5 ± 0.3 |
| | 16 | 370 ± 15 | 381 ± 11 | 319 | 83 ± 2 | 4 | 161.3 ± 0.1 | 146 ± 1 | 2.5 ± 0.2 |
| | 24 | 365 ± 05 | 367 ± 02 | 370 | 80 ± 2 | 5 | 162.5 ± 1.1 | 143 ± 1 | 2.7 ± 0.1 |
| P123 (with SB) | 8 | 375 ± 22 | 376 ± 21 | 358 | 51 ± 3 | 3 | 164.9 ± 1.7 | 162 ± 3 | 2.4 ± 0.1 |
| | 16 | 383 ± 36 | 321 ± 09 | 354 | 48 ± 2 | 5 | 165.4 ± 0.8 | 161 ± 2 | 2.8 ± 0.1 |
| | 24 | 368 ± 13 | 374 ± 13 | 372 | 40 ± 3 | 4 | 163.6 ± 0.5 | 164 ± 2 | 2.7 ± 0.1 |

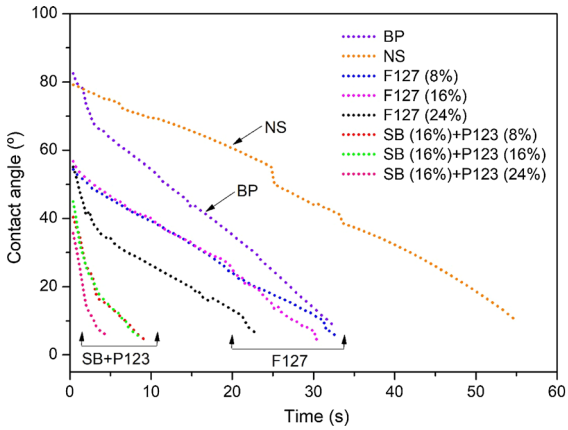


**Fig. 5** Effect of Pluronics (P123 and F127) on the dynamic contact angle

and AKD were always added after cooling down the starch solution to 50 °C. It should also be stressed that P123 and F127 have critical micelle concentrations of 0.313 mM (20 °C) and 0.56 mM (25 °C), respectively. These values are lower than the concentration of Pluronics used in the experiments reported here; additionally, the critical micelle temperatures of these surfactants are well below 50 °C, which also support the idea that Pluronics are found as micelles (He and Alexandridis 2018).

TGA contributes to understand the adsorption of Pluronics in the presence of a cationic polymer. Figure 6 represents the TGA and DTG curves of dip-coated paper samples. It can be seen that the major decomposition areas can be divided into three zones, 275–350 °C, 300–350 °C and 325–400 °C for SB coatings, filter papers and Pluronics coatings, respectively. Interestingly, an increase in the major decomposition area of both Pluronics was observed when filter papers were coated with SB and Pluronics, indicating that the former favors the adsorption of the latter.

## Paper printing properties

### *Gamut area*

It was observed that the GA, presented in Fig. 7a, increased by 8.6%, 9% and 12.5% using 8%, 16% and 24% dry solids content of SB, respectively, compared

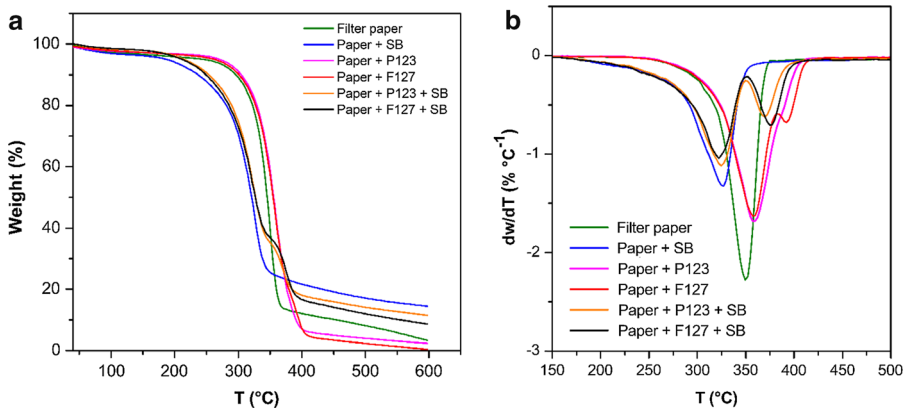


**Fig. 6** TGA (**a**) and DTG (**b**) curves for filter paper, paper + SB, paper + P123, paper + F127, paper + P123 + SB and paper + F127 + SB

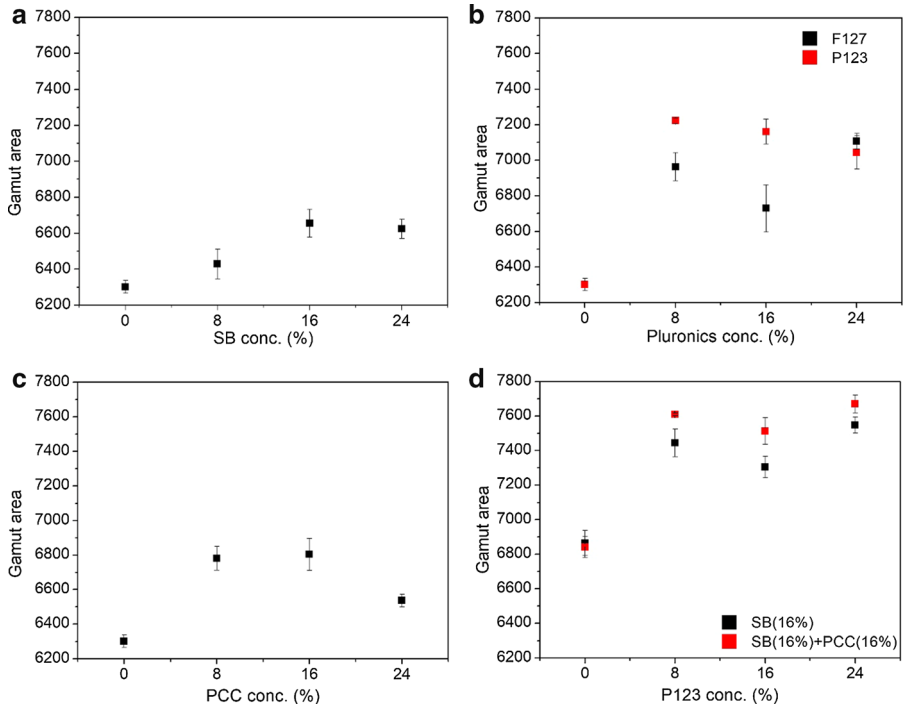


**Fig. 7** Effect of different concentrations of SB (**a**), Pluronics (**b**), PCC (**c**), and their combinations (**d**) on GA

to NS coating. Plausibly, the high DS led to higher deposition of SB on the paper surface, resulting into improved GA (Gigac et al. 2016b; Niegelhell et al. 2018).

Similar to GA, GV, which considers the color luminance *L*, besides *a* and *b*, also increased with increasing SB concentration. The maximum increase was 16.4%, using 24% of SB, compared to NS coating (Table 3).

In Fig. 7b, the GA for different concentrations of Pluronics P123 and F127 is presented. GA was improved by 14.6% using 8% of P123 in the coating solution; however, the GA was further reduced by increasing the P123 concentration from 8 up to 24%. For F127, the 8% addition improved the GA by 10.5%, but further increase in the concentration of F127, from 8 up to 16%, reduced the GA as well. However, the use of 24% of F127 showed almost equal GA increase as

24% of P123, 11.8% and 12.8%, respectively. The increase of GA can be explained by the amphiphilic nature of Pluronics, which facilitates the strong adsorption of these components on cellulosic surfaces (Liu et al. 2010). Additionally, Pluronics form inclusive complexes with starches, leading to the formation of self-supporting flocs in the coating formulation, and enhancing the dispersion of other coating components (Petkova-Olsson et al. 2016, 2017). Remarkably, the lowest amount of P123 and F127 (8%) was found to be more favorable to improve GA. This area was also improved by ∼ 7.9% in the presence of PCC at a concentration of 8% or 16% (Fig. 7c), which is related to the gain in hydrophobicity of the paper surface. However, roughness increased with the presence of PCC and GA was further decreased by 3.7% with a large content of PCC (24%) in the coating formulation.

The effect of P123 coatings in combination with SB (16%) and SB (16%)/PCC (16%) is displayed in Fig. 7d. It is observed that GA increases by 8.5–9% using P123 or a mixture of P123 and PCC. It was further improved significantly by 16–20% and 19–22% with the presence of SB/P123 and SB/P123/PCC, respectively. This enhancement can be explained by the sorption of Pluronics on the cellulosic surface, which increases in combination with a highly cationic polymer (Liu et al. 2011, 2010). Moreover, formation of amylose-Pluronics inclusion complexes may also facilitates the immobilization of the ink pigments on the coated paper surface, improving GA.

*Optical density*

Figure 8 presents the OD of the black color with increasing concentration of SB (A), Pluronics (B), PCC (C) and SB/P123/PCC (D). Figure 8c shows the effect of PCC concentration on OD. OD for PCC coating correlates with the Gurley permeability, attaining deeper tones as the sheet became more resistant to air flow (Kasmani et al. 2013). The highest improvement was observed at 8% of PCC. Likewise, OD followed the same trends as GA, and thus it increased with increasing concentration of SB and P123/F127. Above all, Fig. 8d shows that the highest increase in OD was achieved with the combination of SB-P123-PCC in the coating formulation.

*Inter-color bleed (ITCB), print-through (PT) and circularity for black color*

Figure 9 presents the ITCB, PT and circularity (black dots) of SB, PCC, P123, SB/P123 and SB/P123/PCC coated papers. Similar to GA, ITCB was also improved (*i.e.*, reduced) upon the addition of these components. The highest decrease in ITCB, 15.9%, was observed with SB/P123/PCC coatings. Unlike GA and ITCB, PT of SB/P123 or SB/P123/PCC-coated paper showed a higher PT at the concentrations used in this work, due to decrease in viscosity of the coating formulation, letting the formulation go deeper into the cellulose matrix, which increased the show-through of ink from the other (non-coated) side of the paper. The presence of PCC on the cellulosic surface provided a better improvement in the PT compared to SB or P123 coated papers. Circularity of black dots generally correlates with the ITCB, improving with the formulation containing SB and P123, due to better fixation of ink particles onto the surface.

*Whiteness and fluorescence quenching*

Whiteness, positively correlated with ISO brightness, represents a paper´s ability to equally reflect a balance of all wavelengths of light across the visible spectrum (Hu et al. 2017). The addition of OBA on the paper surface is a cost-effective solution in papermaking to increase the whiteness of printing and writing papers (Shi et al. 2012). Therefore, the interaction between OBA and the other coating components is important. From Table 4, it can be noted that the presence of OBA improved the whiteness of the coated paper but the presence of HCS quenched this agent, resulting in lower whiteness (Fig. S2). It is also worth mentioning that the presence of P123 and PCC did not show any further improvement in the whiteness.

In comparison to NS coatings, whiteness increased by 11% with the addition of OBA. As aforementioned, HCS (with OBA) reduced the whiteness of coated papers by ∼ 10.85% due to the OBA quenching, irrespective of the presence of any other components. Interestingly, such loss of whiteness was not observed when SB was used instead of the cationic starch ether (Fig. S2).

To understand the OBA quenching effect in the presence of HCS and SB, fluorescence emission spectra were recorded for solutions containing OBA

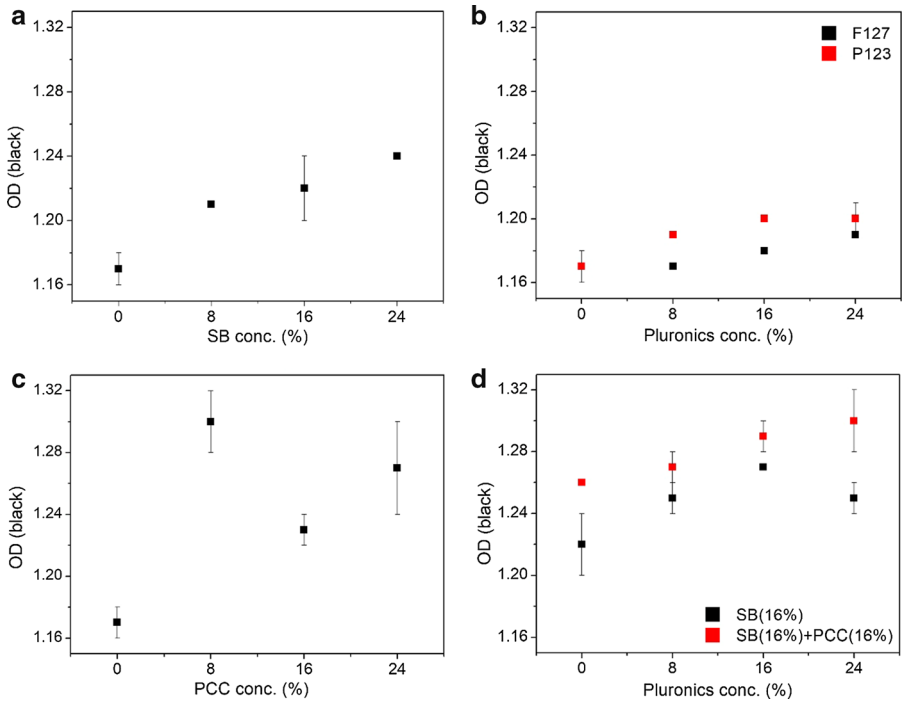


**Fig. 8** Effect of different concentrations of SB (**a**), Pluronics (**b**), PCC (**c**) and their combinations (**d**) on OD (0%: reference coating using NS)

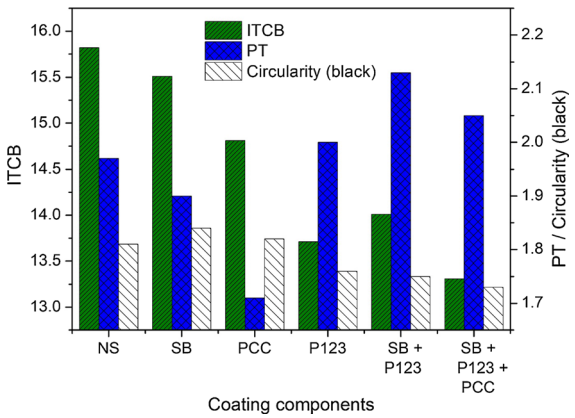


**Fig. 9** Effect of different coating components on ITCB, PT and circularity of black color

(1.84 ppm) and either cationic starch (6.1 ppm), so as to keep the same ratio as in coating formulations (6% OBA/16% CS). Fluorescence quenching was clear in the presence of all cationic starches but, in the case of HCS, the intensity of the emission of blue light ($\sim$ 440 nm) decreased almost by a factor of 4 (Fig. 10).

Quenching was possibly due to the formation of a non-fluorescent complex, where the sulfonate groups of OBA donate electrons to the quaternary ammonium groups of HCS. Still, the most plausible explanation is the aggregation-caused quenching, where aggregation is promoted by electrostatic interactions. The reason for this is that solutions at higher concentration, such as 9.2 ppm OBA/24.4 ppm HCS, showed Rayleigh scattering to such extent that no reliable spectrum could be obtained, even though a concentration of 24.4 ppm lies much below the solubility limit of HCS. In other words, there was a phase transition from solution to dispersion when both solutions, each of them displaying negligible light scattering, were mixed. However, regardless of the quenching mechanism, neither this aggregation nor that extent of quenching was observed when using SB/OBA at the same concentrations, supporting the previously described retention of paper whiteness. Given that SB and HCS had the same DS, it may be concluded that the cationic starch ester possesses a key advantage over its ether counterpart. This advantage should, undoubtedly, be further explored.

**Table 4** Study of interactions among factors. Percentages are related to the total solids content (on the basis of dry weight) of coating formulations

| HCS (%) | P123 (%) | PCC (%) | OBA (%) | GA | OD (cyan) | OD (magenta) | OD (yellow) | OD (black) | PT | ITCB | Circularity (black) | Whiteness |
|---|---|---|---|---|---|---|---|---|---|---|---|---|
| 0 | 0 | 0 | 0 | 6512 | 0.76 | 0.87 | 1.31 | 1.23 | 1.6 | 15.5 | 1.95 | 146 |
| 0 | 0 | 0 | 6 | 6301 | 0.74 | 0.84 | 1.31 | 1.17 | 1.97 | 15.8 | 1.81 | 162 |
| 0 | 0 | 16 | 0 | 6596 | 0.76 | 0.88 | 1.33 | 1.20 | 1.56 | 15.4 | 1.98 | 146 |
| 0 | 0 | 16 | 6 | 7074 | 0.80 | 0.91 | 1.36 | 1.21 | 1.76 | 14.4 | 1.81 | 162 |
| 0 | 16 | 0 | 0 | 6758 | 0.79 | 0.89 | 1.33 | 1.22 | 1.76 | 14.5 | 1.80 | 146 |
| 0 | 16 | 0 | 6 | 6922 | 0.80 | 0.90 | 1.34 | 1.20 | 1.86 | 13.7 | 1.76 | 162 |
| 0 | 16 | 16 | 0 | 7004 | 0.81 | 0.90 | 1.34 | 1.20 | 1.80 | 14.2 | 1.74 | 146 |
| 0 | 16 | 16 | 6 | 6802 | 0.81 | 0.90 | 1.33 | 1.21 | 1.69 | 14.0 | 1.71 | 163 |
| 8 | 8 | 8 | 3 | 7122 | 0.82 | 0.90 | 1.34 | 1.19 | 1.65 | 13.8 | 1.80 | 148 |
| 8 | 8 | 8 | 3 | 7212 | 0.82 | 0.91 | 1.33 | 1.20 | 1.69 | 14.2 | 1.81 | 147 |
| 16 | 0 | 0 | 0 | 6610 | 0.80 | 0.78 | 1.33 | 1.25 | 1.99 | 16.0 | 1.79 | 144 |
| 16 | 0 | 0 | 6 | 6656 | 0.74 | 0.77 | 1.37 | 1.24 | 1.78 | 16.2 | 1.79 | 145 |
| 16 | 0 | 16 | 0 | 6971 | 0.77 | 0.88 | 1.31 | 1.20 | 1.82 | 15.6 | 1.95 | 144 |
| 16 | 0 | 16 | 6 | 6739 | 0.79 | 0.78 | 1.31 | 1.23 | 1.82 | 15.6 | 1.84 | 146 |
| 16 | 16 | 0 | 0 | 7479 | 0.83 | 0.92 | 1.36 | 1.22 | 1.80 | 12.7 | 1.83 | 146 |
| 16 | 16 | 0 | 6 | 7443 | 0.86 | 0.85 | 1.50 | 1.42 | 1.66 | 16.3 | 1.89 | 146 |
| 16 | 16 | 16 | 0 | 7427 | 0.83 | 0.91 | 1.35 | 1.20 | 1.72 | 13.9 | 1.76 | 145 |
| 16 | 16 | 16 | 6 | 7670 | 0.85 | 0.93 | 1.37 | 1.22 | 1.84 | 13.2 | 1.71 | 148 |

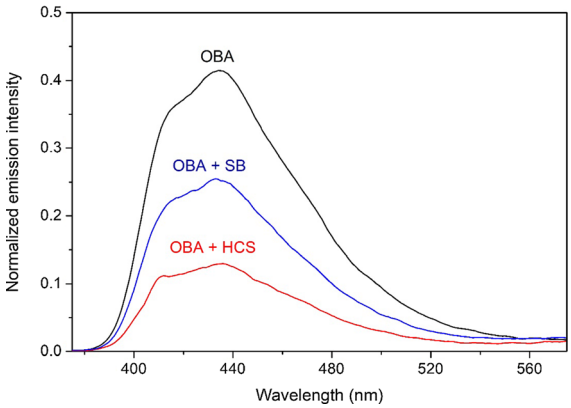


**Fig. 10** Fluorescence emission spectrum of OBA in presence of HCS and SB. An excitation wavelength of 350 nm was used to record all spectra

*Statistical analysis*

Under the hypothesis that the presence of HCS, P123, PCC and OBA in coating formulations would have a positive influence on printing quality parameters, TIBCO's Statistica software allowed to discriminate between those four factors. An in-depth and detailed assessment can be found in the Supplementary Information, including different statistical parameters (such as Fisher–Snedecor's F, Student's t, and β probability) and model validation plots.

Briefly, after processing the results of Table 4, the most relevant variables for the improvement of GA were found to be HCS concentration ($p = 0.005$), P123 concentration ($p = 0.0006$), and their binary interaction ($p = 0.05$). The presence of PCC and OBA and their interactions with other variables did not significantly affect the GA. Regarding OD for cyan, influential factors were, once again, the concentrations of HCS ($p = 0.04$) and P123 ($p < 0.0003$). Nonetheless, the OD for magenta was only influenced in a significant way by P123 ($p = 0.005$). Likewise, only P123 ($p < 0.005$) exerted a significant impact on ITCB. For whiteness, the most significant effect was provided by OBA ($p < 0.001$), HCS and their interaction.

An alternative experimental design, considering three levels for each factor (instead of two), resulted in

significant correlations for the OD of yellow, the OD of black and circularity (Table S1), three responses for which the aforementioned model failed to do so. For instance, circularity was found to be significantly improved by P123 ($p < 0.0005$) and OBA ($p < 0.02$). Other than that, there was a high degree of agreement with the two-level case, highlighting the importance of HCS and P123.

## Conclusions

The effect of an unconventional combination of coating components, highly substituted cationic starch and Pluronics, on the printing quality of office papers was investigated. As a key novelty, cationic starch refers not only to its typical ether form, but also to starch betainate, an ester that has been suggested for bulk addition in sheet forming but not (as far as the authors are concerned) for paper coating. A 24% coating weight of starch betainate increased the gamut area by 12.5%, whilst Pluronics P123 and F127 (8% coating weight) attain improvements of 14.6% and 11.8%, respectively. Both cationic starches, ether and ester, showed the same outcome for improving the paper printing properties in presence and absence of Pluronics. Nonetheless, while the ether caused a certain loss of whiteness, as it quenches the fluorescence emission of the optical agent, such loss was not found when starch betainate was used. The ability of starch betainate of keeping the whiteness gain of an anionic brightening agent is a key finding of this work.

Remarkably, the statistical analysis indicated that besides the aforementioned individual effects of cationic starch and Pluronics, the binary interaction thereof had a significantly positive influence on the gamut area. Furthermore, the optical density (cyan, magenta, yellow and black), inter-color bleed and circularity were successfully correlated with the independent variables. Overall, the combination of cationic starch and Pluronics, accounting for a total solids content of 16%, was found to exert a great impact on the global printing quality.

**Authors' contributions** All authors made substantial contributions to the conception of the work, the acquisition and interpretation of data, and writing. All authors approve the manuscript. All authors agree to be accountable for all aspects of the work in ensuring that questions related to the accuracy or integrity of any part of the work are appropriately investigated and resolved.

**Funding** This work was carried out under the Project inpactus -innovative products and technologies from eucalyptus, Project N.° 21874 funded by Portugal 2020 through European Regional Development Fund (ERDF) in the frame of COMPETE 2020 n°246/AXIS II/2017. Authors would like to thank the Coimbra Chemical Centre, which is supported by the Fundação para a Ciência e a Tecnologia (FCT), through the projects UID/QUI/00313/2020 and COMPETE. Authors would also like to thank the CIEPQPF—Strategic Research Centre Project UIDB/00102/2020, funded by the Fundação para a Ciência e Tecnologia (FCT). M.S. acknowledges the PhD grant BDE 03|POCI-01-0247-FEDER-021874. R.A. acknowledges the post-doc grant BPD 02|POCI-01-0247-FEDER-021874.

**Availability of data and material** All data are displayed in the article and its electronic supplementary information.

**Code availability** Not applicable.

**Declarations**

**Conflict of interest** The authors declare that there is no conflict of interest and that they do not have competing interests.

**Ethics approval** Not applicable. No studies involving humans and/or animals.

**Consent to participate** Not applicable. No studies involving humans and/or animals.

**Consent for publication** Not applicable. No studies involving humans and/or animals.

## References

Alexandridis P, Holzwarthf JF, Hatton TA (1994) Micellization of poly(ethylene oxide)-poly(propylene oxide)-poly(-ethylene oxide) triblock copolymers in aqueous solutions: thermodynamics of copolymer association. Macromolecules 27:2414–2425

Auzély-Velty R, Rinaudo M (2003) Synthesis of starch derivatives with labile cationic groups. Int J Biol Macromol 31:123–129. https://doi.org/10.1016/S0141-8130(02)00072-7

Baptista JGC, Rodrigues SPJ, Matsushita AFY, Vitorino C, Maria TMR, Burrows HD, Pais AACC, Valente AJM (2016) Does poly(vinyl alcohol) act as an amphiphilic polymer? an interaction study with simvastatin. J Mol Liq 222:287–294. https://doi.org/10.1016/j.molliq.2016.07.025

Bendoraitiene J, Lekniute-Kyzike E, Rutkaite R (2018) Biodegradation of cross-linked and cationic starches. Int J Biol Macromol 119:345–351. https://doi.org/10.1016/j.ijbiomac.2018.07.155

Bollström R, Tobjörk D, Dolietis P, Salminen P, Preston J, Österbacka R, Toivakka M (2013) Printability of functional inks on multilayer curtain coated paper. Chem Eng Process 68:13–20. https://doi.org/10.1016/j.cep.2012.07.007

Gao J, Luo Z, Fu X, Luo F, Peng Z (2012) Effect of enzymatic pretreatment on the synthesis and properties of phosphorylated amphoteric starch. Carbohydr Polym 88:917–925. https://doi.org/10.1016/j.carbpol.2012.01.034

Gigac J, Stankovská M, Opálená E, Pažitný A (2016a) The effect of pigments and binders on inkjet print quality. Wood Res 61:215–226

Gigac J, Stankovska M, Pazitny A (2016b) Influence of the coating formulations and base papers on inkjet printability. Wood Res 61:915–926

Granö H, Yli-Kauhaluoma J, Suortti T, Käki J, Nurmi K (2000) Preparation of starch betainate: a novel cationic starch derivative. Carbohydr Polym 41:277–283

Haack V, Heinze T, Oelmeyer G, Kulicke WM (2002) Starch derivatives of high degree of functionalization, synthesis and flocculation behavior of cationic starch polyelectrolytes. Macromol Mater Eng 287:495–502

He Z, Alexandridis P (2018) Micellization thermodynamics of Pluronic P123 (EO20PO70EO20) amphiphilic block copolymer in aqueous ethylammonium nitrate (EAN) solutions. Polymers 10:32. https://doi.org/10.3390/polym10010032

Hebeish A, Higazy A, El-Shafei A, Sharaf S (2010) Synthesis of carboxymethyl cellulose (CMC) and starch-based hybrids and their applications in flocculation and sizing. Carbohydr Polym 79:60–69. https://doi.org/10.1016/j.carbpol.2009.07.022

Hu G, Fu S, Chu F, Lin M (2017) Relationship between paper whiteness and color reproduction in inkjet printing. BioResources 12:4854–4866. https://doi.org/10.15376/biores.12.3.4854-4866

Huber KC, BeMiller JN (2001) Location of sites of reaction within starch granules. Cereal Chem 78:173–180. https://doi.org/10.1094/CCHEM.2001.78.2.173

Kasmani JE, Mahdavi S, Alizadeh A, Nemati M, Samariha A (2013) Physical properties and printability characteristics of mechanical printing paper with LWC. BioResources 8:3646–3656. https://doi.org/10.15376/biores.8.3.3646-3656

Lamminmäki TT, Kettle JP, Gane PAC (2011) Absorption and adsorption of dye-based inkjet inks by coating layer components and the implications for print quality. Colloid Surf A 380:79–88. https://doi.org/10.1016/j.colsurfa.2011.02.015

Lee HL, Shin JY, Koh CH, Ryu H, Lee DJ, Sohn C (2002) Surface sizing with cationic starch: its effect on paper quality and the papermaking process. Tappi J 1:34–40

Liu X, Wu D, Turgman-Cohen S, Genzer J, Theyson TW, Rojas OJ (2010) Adsorption of a nonionic symmetric triblock copolymer on surfaces with different hydrophobicity. Langmuir 26:9565–9574. https://doi.org/10.1021/la100156a

Liu X, Vesterinen AH, Genzer J, Seppälä JV, Rojas OJ (2011) Adsorption of PEO-PPO-PEO triblock copolymers with end-capped cationic chains of poly(2-dimethylaminoethyl methacrylate). Langmuir 27:9769–9780. https://doi.org/10.1021/la201596x

Lourenço AF, Gamelas JAF, Sarmento P, Ferreira PJT (2020) Cellulose micro and nanofibrils as coating agent for improved printability in office papers. Cellulose 27(10):6001–6010. https://doi.org/10.1007/s10570-020-03184-9

Mujawar LH, Van Amerongen A, Norde W (2015) Influence of Pluronic F127 on the distribution and functionality of inkjet-printed biomolecules in porous nitrocellulose substrates. Talanta 131:541–547. https://doi.org/10.1016/j.talanta.2014.08.001

Niegelhell K, Chemelli A, Hobisch J, Griesser T, Reiter H, Hirn U, Spirk S (2018) Interaction of industrially relevant cationic starches with cellulose. Carbohydr Polym 179:290–296. https://doi.org/10.1016/j.carbpol.2017.10.003

Petkova-Olsson Y, Ullsten H, Järnström L (2016) Thermosensitive silica-pluronic-starch model coating dispersion-part I: the effect of Pluronic block copolymer adsorption on the colloidal stability and rheology. Colloid Surf A 506:245–253. https://doi.org/10.1016/j.colsurfa.2016.06.032

Petkova-Olsson Y, Altun S, Ullsten H, Järnström L (2017) Temperature effect on the complex formation between Pluronic F127 and starch. Carbohydr Polym 166:264–270. https://doi.org/10.1016/j.carbpol.2017.02.012

Sharma M, Aguado R, Murtinho D, Valente AJM, de Sousa APM, Ferreira PJT (2020) A review on cationic starch and nanocellulose as paper coating components. Int J Biol Macromol 162:578–598. https://doi.org/10.1016/j.ijbiomac.2020.06.131

Sharma M, Aguado R, Murtinho D, Valente AJM, Ferreira PJT (2021) Novel approach on the synthesis of starch betainate by transesterification. Int J Biol Macromol 182:1681–1689. https://doi.org/10.1016/j.ijbiomac.2021.05.175

Shi H, Liu H, Ni Y, Yuan Z, Zou X, Zhou Y (2012) Review: Use of optical brightening agents (OBAs) in the production of paper containing high-yield pulps. BioResources 7:2582–2591. https://doi.org/10.15376/biores.7.2.2582-2591

Sousa S, Mendes de Sousa A, Reis B, Ramos A (2014) Influence of binders on inkjet print quality. Mater Sci 20:55–60. https://doi.org/10.5755/j01.ms.20.1.1998

Stankovská M, Gigac J, Letko M, Opálená E (2014) The effect of surface sizing on paper wettability and on properties of inkjet prints. Wood Res 59:67–76

Thapa RK, Cazzador F, Grønlien KG, Tønnesen HH (2020) Effect of curcumin and cosolvents on the micellization of Pluronic F127 in aqueous solution. Colloid Surf B 195:111250. https://doi.org/10.1016/j.colsurfb.2020.111250

Wang S, Cheng Q (2009) A novel process to isolate fibrils from cellulose fibers by high-intensity ultrasonication, Part 1: process optimization. J Appl Polym Sci 113:1270–1275